Pure & Appl. Chem., Vol. 70, No. 11, pp. 2177–2187, 1998.
Printed in Great Britain.

Interfacial photochemistry: Fundamentals and applications

A. Fujishima and Tata N. Rao

Deapartment of Applied Chemistry, School of Engineering
The University of Tokyo, Hongo, Bunkyo-ku, Tokyo 113-8656, Japan

Abstract: This article deals with the photochemical processes occurring at semiconductor/liquid and semiconductor/gas interfaces and gives an overview of fundamentals and applications of TiO_2 photocatalysis together with the photoelectrochemical characterization of diamond thin films and azobenzene derivative (ABD) monolayers. The first part of this paper discusses the TiO_2 photocatalysis with a special emphasis on kinetic aspects of photocatalysis under very low and relatively high UV intensities as well as a wide range of initial concentrations of reactants. The second part deals with a novel photoinduced super amphiphilic TiO_2 surface which has a wide potential applications. In the third part, we present our recent work on the photoelectrochemistry of the semiconducting diamond/electrolyte interface including the influence of the surface conditions on the interfacial electron transfer properties. The last part of this article includes the photoelectrochemistry of azobenzene derivative monolayers that exhibit unusual redox behavior in aqueous solution.

INTRODUCTION

It was recognized a long time ago that light-activated semiconductors can trigger many kinds of reactions without participating directly. Our discovery of photoinduced water splitting on TiO_2 electrodes (ref. 1) has promoted extensive research on TiO_2 and other semiconductor materials, which have been widely adopted as potential materials for solar energy conversion (ref. 2-5). A schematic of the cell used in our first experiment is shown in Fig. 1. Upon illumination of the TiO_2

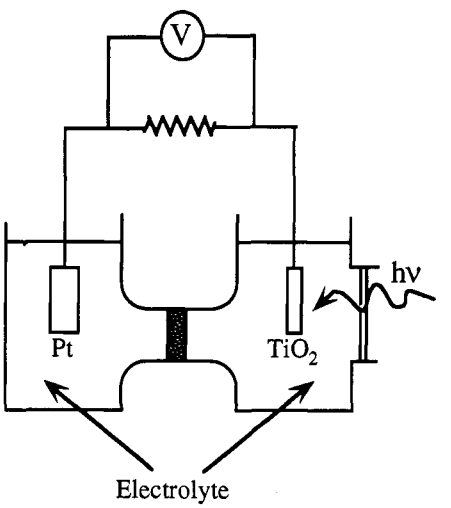

Figure 1. A photoelectrochemical cell consisting of TiO_2 and Pt electrodes in an aqueous electrolyte

*Lecture presented at the 17th IUPAC Symposium on Photochemistry, Sitges, Barcelona, Spain, 19–24 July 1998. Other presentations are published in this issue, pp. 2147–2232.

anode, current flow from the Pt electrode to the TiO_2 electrode was observed in an aqueous solution, indicating evolution of oxygen gas at the TiO_2 electrode and evolution of hydrogen at Pt electrode. The photoelectrochemical reaction is a result of photogenerated electrons and holes in the conduction and valence bands, respectively. The reaction scheme involving the photogenerated electron and hole can be written as follows:

$$TiO_2 + 2h\upsilon \longrightarrow 2e^- + 2h^+$$
$$H_2O + 2h^+ \longrightarrow 1/2\ O_2 + 2\ H^+ \text{ (at the } TiO_2 \text{ electrode)}$$
$$2H^+ + 2e^- \longrightarrow H_2 \text{ (at the Pt electrode)}$$

This work also revealed the potential use of TiO_2 for the photocatalytic oxidation of many organic substrates, which is interesting from the point of view of environmental purification. This is due to the fact that the oxidation potential of TiO_2 (3.0 V vs SCE) is considerably higher than that of more conventional oxidizing agents such as chlorine (1.36 V vs SHE) and ozone (2.07 V vs SCE). Furthermore, TiO_2 compatible with many types of practical catalytic systems due to its chemical inertness and non-toxicity.

There have been several reports on the use of TiO_2 as a photocatalyst for various applications such as the recovery of precious metals (ref. 6) and waste water treatment (refs. 7, 8). Heller's group demonstrated the use of TiO_2-coated glass microbubbles in the photodegradation of oil and chemical slicks on water (ref. 9). TiO_2, due to its wide band gap (3.2 V) cannot make use of solar light effectively, as it requires UV light for excitation. Hence, we have paid attention to how to use the weak UV light available in the solar radiation and in ordinary fluorescent lamps, so that the application of photocatalysis in indoor living and working environments becomes more practical. As a result, we succeded in developing transparent TiO_2 coatings on various substrates such as glass (refs. 10, 11) and ceramic tiles (12), which could photodegrade various noxious, malodorous chemicals, smoke residues and cooking oil residues. The photodegradation was observed even under low intensity indoor light. Based on these developments, the Japanese company TOTO has produced such tiles for use in rest rooms and hospitals to maintain bacteria-free environments. We are also collaborating with other companies to produce photocatalytic cover glasses for lighting systems used in tunnels. In addition to photocatalytic properties, TiO_2 films have exhibited amphiphilic surface wettability induced by UV illumination (refs. 15, 16), leading to applications in self-cleaning and anti-fogging glass.

Another interesting material for interfacial photochemistry is semiconducting diamond. Undoped diamond is a good electrical insulator. The resistivity of diamond can be decreased drastically by doping with boron (ref. 17). Highly conductive electrodes were found to exhibit excellent electrochemical characteristics including wide electrochemical potential window, low background currents and high resistance to deactivation (ref. 18). Although, several reports are available on diamond electrochemistry, there are few reports available on the photoelectrochemistry of diamond (refs. 19, 20). We are trying to make use of semiconducting diamond for various photoelectrochemical reduction reactions.

While TiO_2 is a good candidate for photoinduced oxidation reactions, boron doped (p-type) diamond is suitable for photoinduced reduction reactions. As the conduction band of the diamond is located near the vacuum level, the photogenerated electrons in diamond have very high reducing power (ref. 21). These electrons can be trapped by species having highly negative redox potentials. Reactions such as dinitrogen reduction, CO_2 reduction and deposition of electronegative metals are interesting to examine at semiconducting diamond electrodes. We present some of our recent work on the preliminary characterization of the semiconducting diamond /electrolyte interface.

Azobenzene is well known as a photochromic material (ref. 22). It has several applications due to its unique property of photochemical isomerization (refs. 23, 24). The trans isomer of azobenzene is energetically more stable than its cis isomer. It is known that the electrochemical properties of azobenzene can be influenced by photochemical reactions (ref. 25). However, the electrochemistry of azobenzene in aqueous solution is not well understood. In the case of azobenzene derivative (ABD) monolayers, the electrochemical properties are further affected by various structural properties of the layer such as long range electron transfer between electrode and azobenzene. Usually thiol monolayers on gold are effective substrates for ABD monolayers. Hence, the electrochemical properties of an ABD film can be varied by changing the length of the thiol

molecules, which determine the length of the electron pathway. For example, we could observe a difference in reduction potential between cis and trans isomers by changing the length of the thiol molecules (ref. 26). Here, we present some interesting aspects of this work including photoelectrochemistry.

TiO_2 PHOTOCATALYSIS

As mentioned in the introduction, making use of weak UV light available in the sunlight and in room light is one of our interests in TiO_2 photocatalysis. Figure 2 shows a typical example for the efficient photocatalytic decomposition of gaseous acetaldehyde (a malodours gas) on TiO_2-films under low UV light intensities (ref. 27). In this case, the light intensity was 0.4 mW/cm^2. It is important to note that the initial concentration of acetaldehyde in Fig. 2 is only 300 parts per million by volume (ppmv). Usually, foul odors in the indoor environment arise from compounds which are present at a level of only 10 ppmv or so. Hence, the weak UV light available in ordinary fluorescent lighting should be sufficient to decompose such compounds on a TiO_2 surface.

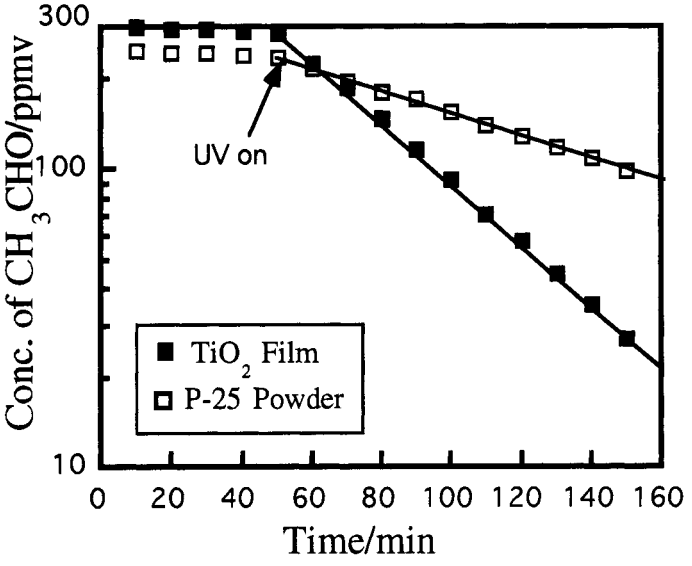

Figure 2. Photocatalytic decomposition of acetaldehyde on various TiO_2 photocatalysts as afunction of time.

Highly transparent photocatalytic TiO_2 thin films were prepared on glass substrates in order to use them as window materials. These films were made via the sol-gel method (ref. 28). The resulting films, with a thickness of ~0.6 mm, showed ~80% transparency in the visible region. Such TiO_2 coated window glasses can make use of both sunlight and room light. Thin films coated on various types of glass substrates were tested for the photocatalytic decomposition of vegetable oil films present on the surfaces. A complete decomposition of the oil was observed on a TiO_2 coated soda-lime glass plate in the presence of an intermediate SiO_2 layer. In the absence of such SiO_2 coating, the TiO_2 films did not show high activity, probably due to the diffusion of Na^+ ions from the soda-lime glass to the TiO_2 layer, resulting in the formation of inactive $NaTiO_3$ during the film preparation. Such transparent films can be coated on other indoor materials such as tiles, so that the original colors and designs are not affected.

TiO_2-containing composite materials are also interesting for indoor applications. For example, TiO_2-containing papers were developed to examine their photocatalytic activity (ref. 29). The photocatalytic activity of these papers was investigated by measuring the decomposition of gaseous acetaldehyde using a conventional white fluorescent light. The films were found to be highly efficient, the efficiency being much higher than that of Degussa P-25, one of the most efficient commercial TiO_2 powders. Table 1 summarizes the quantum yields for paper containing various

amounts of TiO_2, including the data obtained on P-25 powder. A quantum yield of 90% was obtained with TiO_2-containing paper, the value being two times higher than that of P-25 (43%) These results indicate the suitability of paper pulp as a matrix for TiO_2. These TiO_2-containing papers were found to be stable, as the UV light intensity from a white fluorescent bulb is rather weak.

In addition to the high activity for photocatalytic decomposition of organic substrates, TiO_2 was also shown to exhibit good anti-bacterial activity under illumination (ref. 30). Sterilization experiments using TiO_2 have shown excellent results. Figure 3 shows the percentage survival ratio of *Escherichia coli (E. coli)* in a liquid film under different conditions as a function of time. The experiment was carried out under UV light illumination with an intensity of 1 mW/cm^2. The survival ratio for *E. coli* in the liquid film on the TiO_2 decreased to a negligible level within 1 h. In the absence of TiO_2, UV illumination caused only 50% sterilization within 4 h. Thus, we have succeeded to make use of TiO_2 effectively under weak UV light conditions. Our studies have also revealed that photoproduced $\cdot OH$ and O_2^- species participate in the anti-bacterial effect. Today, several types indoor building materials are available for sterilization applications. In addition, TiO_2 has been found to be useful for the photocatalytic destruction of T24 cancer cells (ref. 31).

Table 1. Quantum yields for the decomposition of gaseous acetaldehyde, using photocatalytic papers with various amounts of added TiO_2 and P-25 powder.

Sample	Quantum yield(%)		
	Φ_{CH_3COOH}	Φ_{CO_2}	Φ_{total}
TiO_2-containing (2 wt%) sheet	14	10	24
TiO_2-containing (5 wt%) sheet	15	27	42
TiO_2-containing (10 wt%) sheet	58	32	90
P-25 powder	37	6	43

UV intensity: 0.50 mW/cm^2; initial concentration of CH_3CHO: 1000ppm.

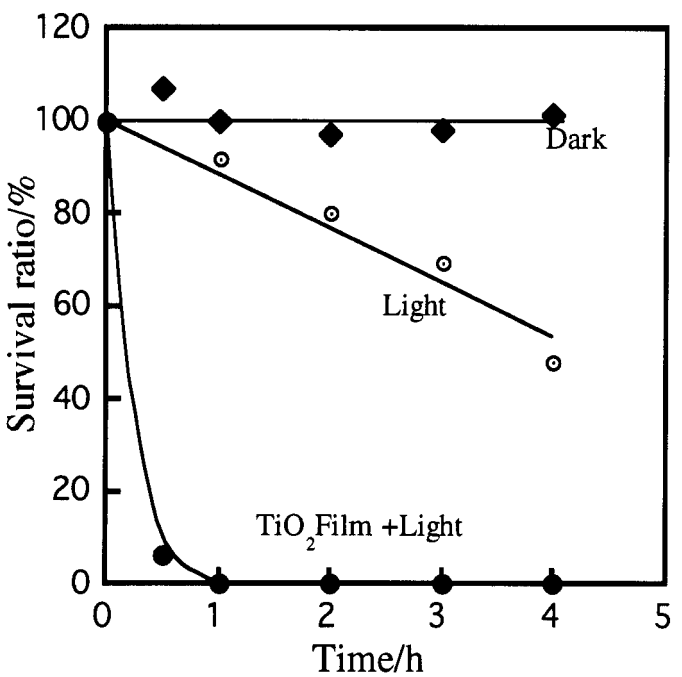

Figure 3. Survival ratio of E. coli in the presence and absence of TiO_2 film under weak UV irradiation.

In order to investigate the kinetics of the stationary photocatalytic decomposition of dilute gases under low-intensity UV illumination, we have selected gas-phase 2-propanol as a model compound (refs. 32, 33). The reason for the selection of 2-propanol is that it decomposes to acetone, which undergoes further reactions at relatively slower rates. Since the production of acetone involves absorption of one photon per molecule, the apparent quantum yield (QY) values could be calculated from the ratio of the number of generated acetone molecules/number of absorbed photons. The values of QY for a propanol concentration of 1000 ppmv were found to increase with decreasing numbers of absorbed photons and finally saturated at a value of ~28%, indicating that purely light-limited condition were reached. Even for lower initial concentrations, the QY values reached same maximum at lower light intensities. The incident light intensity used in this study ranged from 36 nW/cm^2 to 45μW/cm^2.

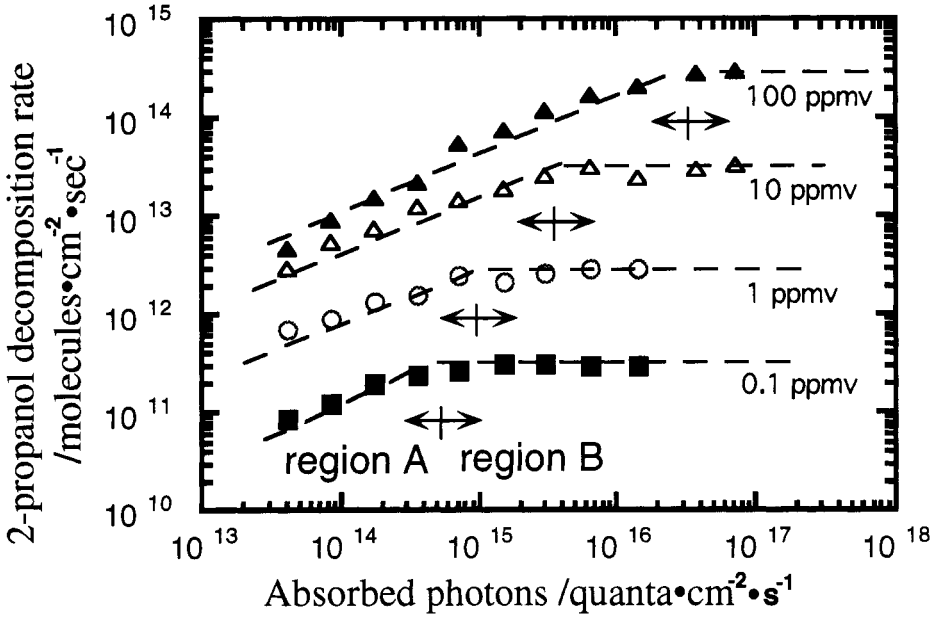

Figure 4. Dependence of 2-propanol decomposition rate on the number of absorbed photons per unit time.

A similar study was carried out at relatively high intensities (35 μW/cm^2 - 60 mW/cm^2). In this study, the degradation rate of 2-propanol was found to increase with increasing numbers of absorbed photons and gradually saturated, indicating the attainment of mass transport-limited conditions (Fig. 4). We have simulated the decrease in gas-phase 2-propanol concentration as a function of time under mass transport-limited conditions using the one-dimensional diffusion equation. Based on these results, we have mapped various regions on a light intensity vs. initial reactant concentration plot, showing pure mass transport-limited conditions and pure light intensity-limited conditions (Fig. 5). It is pertinent to note that the plot covers 6 orders of magnitude of reactant concentration and 8 orders of magnitude of light intensity.

The general mechanism for the TiO_2 photocatalysis involves the oxidation of surface hydroxyl groups, which participate in the photocatalytic oxidation process. Although direct oxidation of substrates by photogenerated holes is possible, the involvement of •OH in the oxidation process has gained much experimental support. To drive the photocatalytic reaction and maintain charge neutrality, oxygen undergoes reduction in aerated aqueous media, resulting in the formation of O_2• and H_2O_2, which in turn participate in further oxidation processes. Heller et al. (ref. 34) suggested that, although, photogenerated valence band holes initiate the process, the actual oxidizer is molecular oxygen. The production of H_2O_2 is possible also via coupling of •OH radicals. The relative extent of these various reactions cannot be determined by conventional methods. However, we have succeeded in developing a microsensor for the detection of catalytic products in different microscopically localized areas of model photocatalyst surfaces. Using a "wired" horseradish peroxide microelectrode sensor, positioned close to a surface of a TiO_2-ITO (indium tin oxide) composite film, H_2O_2 production via photogenerated hole-mediated oxidation of water and

photogenerated electron-mediated reduction of oxygen were monitored independently (ref. 35). It was found that the majority of H_2O_2 was produced via reduction on the ITO portion. This observation indicated that H_2O_2 was produced mostly by reduction of dissolved oxygen, rather than by oxidation of water, even in the absence of an electron donor.

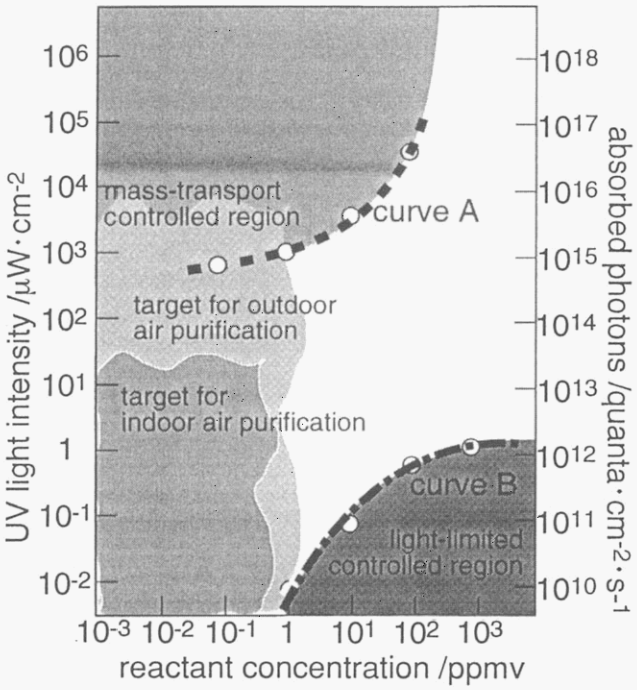

Figure 5. Plot of light intensity vs initial concentration showing mass-transport and light limiting regions.

By using a microelectrode system we could also monitor the consumption of oxygen in the photocatalytic decomposition of ethanol at Pd (reduction) and TiO_2 (oxidation) sites separately on a Pd-TiO_2 composite film (ref. 36). These results indicated that the consumption of O_2 above TiO_2 sites is not due to O_2 reduction but due to the addition of O_2 to α–radicals as shown in the following reactions.

$$H_2O + h^+ \longrightarrow \cdot OH + H^+$$
$$\cdot OH + CH_3CH_2OH \longrightarrow CH_3C\cdot HOH + H_2O$$
$$CH_3C\cdot HOH + O_2 \longrightarrow CH_3CH(OH)OO\cdot$$
$$CH_3CH(OH)OO\cdot \longrightarrow CH_3CHO + O_2\cdot^- + H^+$$
$$CH_3CH(OH)OO\cdot + CH_3CH_2OH \longrightarrow CH_3CH(OH)OOH + CH_3C\cdot HOH$$
$$CH_3CH(OH)OOH \longrightarrow CH_3CHO + H_2O_2$$

Further studies (ref. 37) were carried out to examine the role of superoxide radicals in the photocatalytic decomposition of ethanol. We found an increase in the rate of decomposition of ethanol due to superoxide radicals. From these studies, we proposed that the superoxide radicals react with the 1-hydroxyethylperoxyl radicals generated in the above reactions to form unstable tetraoxides.

$$CH_3CH(OH)OO\cdot + O_2\cdot^- \longrightarrow CH_3CH(OH)OOO^-$$

The resulting tetraoxide is expected to decompose to radicals or non-radical products.

PHOTOINDUCED AMPHIPHILIC TiO_2 SURFACES

The wettability of a surface depends on the nature of the material and surface conditions. For example, the wettability of an oxide surface may change from hydrophilic to hydrophobic when it is exposed to the atmosphere for long time, due to the adsorption of organic contaminants on the

surface. It is interesting to develop methods to control the surface wettability of a solid substrate in view of various practical applications. With this view, we have studied the photo-controlled surface wettability of TiO_2 films and single crystals. As a result we could develop a photoinduced amphiphilic TiO_2 surface (refs. 15, 16).

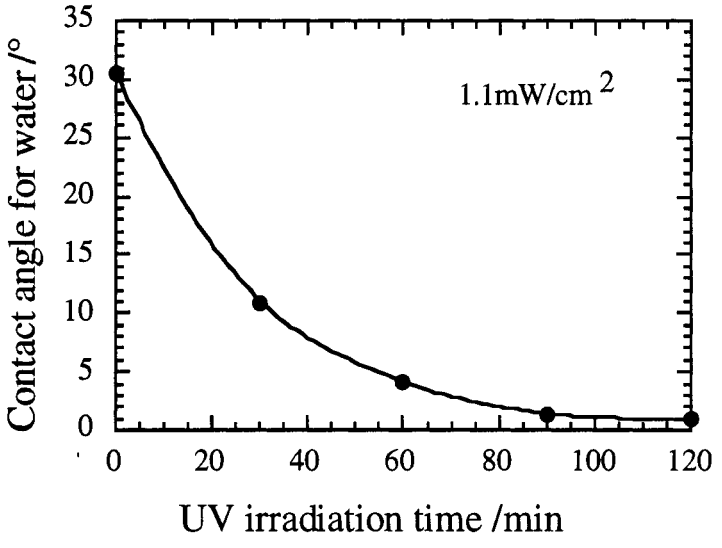

Figure 6. Effect of UV irradiation on the water contact angle

Figure 6 shows the contact angle for water on a freshly prepared TiO_2 film on glass as a function of time under UV irradiation. The film showed a water contact angle of 30° before irradiation. After irradiation with weak UV light (1.1 mW/cm^2), the water contact angle slowly decreased and finally reached a value of ~0°. A rapid decrease in contact angle was observed at higher light intensities. These results demonstrated the antifogging effect under UV illumination. Such an effect can be seen in Fig. 7. The freshly prepared TiO_2 film on a glass substrate fogs when it is exposed to water vapor (Fig. 7a). After UV illumination, the glass becomes transparent, as evident from the clear visibility of the text on the paper placed below the glass (Fig. 7b). Surprisingly, drastic reductions in contact angle under UV illumination have also been observed with oils, indicating the photogeneration of an amphiphilic surface.

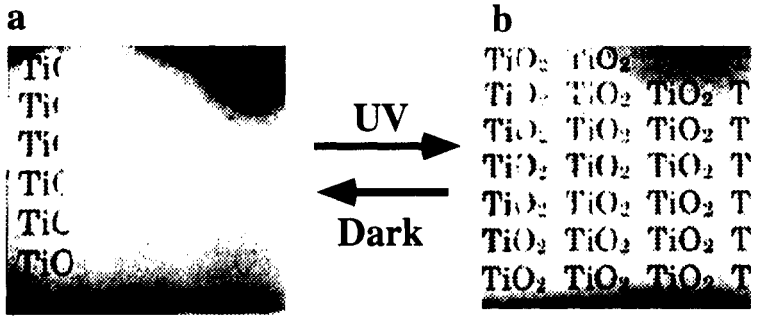

Figure 7. (a) A hydrophobic TiO_2 surface exposed to water vapour.
(b) Generation of an antifogging surface bu UV irradiation.

Although it was thought initially that the wettability change was due to the photocatalytic decomposition of contaminants on the surface, our further studies indicated that it was due to the photogeneration of defect sites on the TiO_2 surface. Friction force microscopic (FFM) measurements on rutile TiO_2 (110) single crystals have indicated the formation of microscopic

domains corresponding to hydrophilic and hydrophobic areas due to UV irradiation. Oxygen vacancies are likely to be created at two-coordinated bridging sites, resulting in the conversion of Ti^{4+} site to Ti^{3+} sites, which are favorable for dissociative water adsorption. Adsorbed water on the hydrophilic domains was confirmed by XPS. For further evidence, the water contact angle on a TiO_2 film was observed in the dark under exposure of O_2 gas. A rapid increase in the contact angle was observed, which can be attributed to the healing of Ti^{3+} defect sites. These conclusions were further supported by FTIR measurements.

Such transparent, highly amphiphilic surfaces are highly promising for practical applications. The involvement of TiO_2 makes these surfaces more promising due to its photocatalytic self-cleaning property. In order to demonstrate this fact, we have suspended TiO_2 coated and uncoated ceramic tiles in the outdoor atmosphere for six months. The TiO_2-coated tiles remained clean as expected. This result also indicates that the UV illumination from sunlight is sufficient to create the amphiphilic surface so that hydrophilic or oleophilic contaminants on the surface can be easily removed by rain. Our industrial collaborator TOTO is developing various commercial products based on this technology.

PHOTOELECTROCHEMISTRY OF SEMICONDUCTING DIAMOND

As mentioned before, the photoelectrochemistry of diamond is interesting, in part because the photogenerated electrons in the conduction band of diamond have very high reducing power. After the development of the chemical vapor deposition (CVD) method, it has become easy to grow diamond films on various substrates. The microwave plasma CVD method produces very high quality diamond films. High quality diamond films are required for photoelectrochemical characterization because the presence of any non-diamond impurities on the film can influence the PEC properties of diamond. Earlier, photocurrents due to sub-band gap illumination were reported and these were probably produced due to impurities (refs. 19, 20). Recently, we succeeded in obtaining high quality diamond films and demonstrated the generation of photocurrents in weakly UV-absorbing aqueous electrolytes under supra-band gap illumination (ref. 21).

In addition to the problems with non-diamond carbon impurities, the surface condition of diamond also influences the photoelectrochemical properties. Usually, as-grown diamond is hydrophobic due to the hydrogen termination of the surface. Incorporation of oxygen on the surface makes the diamond surface hydrophilic. Such a modification on the surface also influences its electrical and electrochemical properties. Recently, we have investigated the influence of such surface

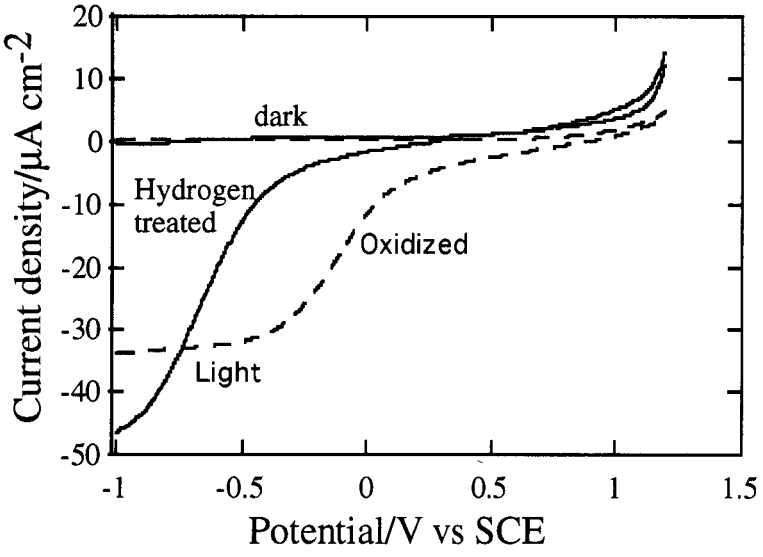

Figure 8. i-V curves for a semiconducting diamond electrode subjected to different treatments.

modification of semiconducting diamond on its photoelectrochemical properties (ref. 38). Figure 8 shows the current-voltage plots for hydrogen plasma-treated and electrochemically oxidized semiconducting diamond electrodes. A significant anodic shift in the onset potential of hydrogen evolution was observed, due to electrochemical oxidation of the surface. This is an interesting observation, because the oxidative treatment could improve the photoelectrochemical properties. Several reasons were suggested for the anodic shift observed in the onset potential. The oxygen functional groups formed on the diamond surface can cause changes in the potential drop in the Helmholtz layer, resulting in a shift in the onset potential. The formation of oxygen groups was confirmed by XPS. A change in the potential drop across a very thin oxide film on the oxidized diamond surface is also possible.

PHOTOELECTROCHEMISTRY OF AZOBENZENE DERIVATIVE (ABD) MONOLAYERS

As mentioned previously, the electrochemical properties of ABD monolayers are dependent on the length of the thiol molecules in the substrate. We have obtained cyclic voltammograms for ABD monolayer films consisting of various lengths of thiol molecules. The layers were adsorbed on the thiol monolayer surface with the hydrophobic alkyl terminal. Trans-ABD monolayer films did not show any faradaic response in the potential region of +0.6 V to -0.6 V vs. Ag/AgCl. However, redox peaks appeared with the cis-isomer due to reduction of to hydrazobenzene derivative (HBD) and the oxidation of HBD to trans-ABD. The cis-isomer was generated by UV irradiation before the experiment. The peak separation was found to increase with increasing length of the thiol molecule, which acts as a spacer between the gold electrode and the ABD molecule. Thus the irreversibility of the redox reaction increases with the length of the thiol molecule, due to the increasing electron transfer path length. To minimize this path length, we have used 2-mercaptoethanol, HOC_2H_4SH, as a spacer, so that the hydrophilic terminal of the ABD molecules adsorbs on the spacer layer (ref. 26). An ideal redox behavior is expected on such film. But, surprisingly, no redox peaks appeared for cis-ABD, which was photogenerated before the cyclic voltammetric experiment. We have explained this observation with a hypothesis based on the idea that the reduction potential of cis-ABD becomes more anodic than the oxidation potential of HBD (Fig. 9). Hence, inversion of the redox potentials of cis-ABD and HBD is suggested. The absence of the redox peaks in the cyclic voltammogram is probably due to the fast electron exchange between the gold electrode and the azo group of ABD layer.

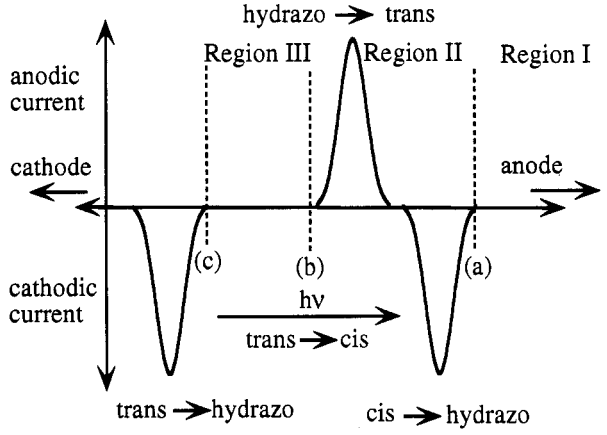

Figure 9. Schematic illustration of redox potentials for trans-ABD reduction, cis-ABD reduction and HBD oxidation.

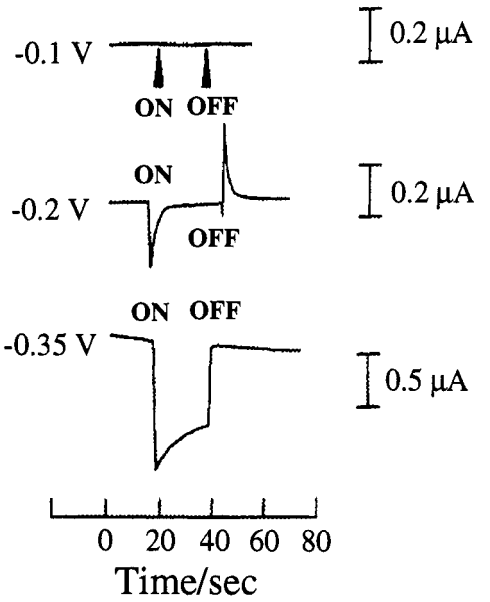

Figure 10. Photocurrent response of the trans-ABD monolayer film deposited on the ethanethiol monolayer by UV light irradiation at cathodic potential bias.

In order to examine our hypothesis, the electrochemical response of the trans-ABD was examined under UV irradiation. UV irradiation generates the cis-isomer. Figure 10 shows the photocurrent response at different potentials, corresponding to three regions indicated in Fig. 9. At a potential of -0.2 V (region II in Fig. 9), a pair of electrical spikes appeared due to UV irradiation. Upon irradiation, a sharp cathodic spike appeared, and, when the light was cut off, an anodic spike appeared. Both spikes decayed rapidly to their original positions. Such spikes were not observed in regions I and II. These observations indicate the simultaneous reduction and oxidation reactions of the cis-isomer at this potential. Further evidence for this hypothesis was obtained from fast scan voltammetry. At a scan rate of 500 mV/s, we could obtain a cyclic voltammogram showing both anodic and cathodic peaks, confirming the inversion of the redox potentials (ref. 39).

REFERENCES

1. A. Fujishima, K. Honda. Nature **238**, 37 (1972).
2. A. Heller. Acc. Chem. Res. **14**, 154 (1981).
3. A. Heller. Science **223**, 1141 (1984).
4. S. Licht, D. Peramunage. Nature **345**, 330 (1990).
5. B. O'Regan, M. Grätzel. Nature **353**, 737 (1991).
6. T.-K. Li, Y.-N. Zu, X.-R. Xiao, G.-D. Zhou, X.-P. Li, A. Fujishima. Acta Energiae Solaris Sinica **7**, 188 (1986).
7. R. W. Matthews. J. Catal. **111**, 264 (1988).
8. A. Mills, R. H. Davies, D. Worsley. Chem. Soc. Rev. 417 (1993).
9. I. Rosenberg, J. R. Brock, A. Heller. J. Phys. Chem. **96**, 3423 (1992).
10. I. Sopyan, S. Murasawa, K. Hashimoto, A. Fujishima. Chem. Lett. 723 (1994).
11. I. Sopyan, M. Watanabe, S. Murasawa, K. Hashimoto, A. Fujishima. J. Photochem. Photobiol. A: Chem. **98**, 79 (1996).
12. T. Watanabe, A. Kitamura, E. Kojima, C. Nakayama, K. Hashimoto, A. Fujishima. Photocatalytic Purification and Treatment of Water and Air, p. 747. Elsevier, Amsterdam (1993).
13. I. Sopyan, M. Watanabe, S. Murasawa, K. Hashimoto, A. Fujishima. J. Electroanal. Chem. **415**, 183 (1996).

14. I. Sopyan, M. Watanabe, S. Murasawa, K. Hashimoto, A. Fujishima. Chem. Lett. 69 (1996).
15. R. Wang, K. Hashimoto, A. Fujishima, M. Chikuni, E. Kojima, A. Kitamura, M. Shimohigoshi, T. Watanabe. Nature **388**, 431 (1997).
16. R. Wang, K. Hashimoto, A. Fujishima, M. Chikuni, E. Kojima, A. Kitamura, M. Shimohigoshi, T. Watanabe. Adv. Mater. **10**, 135 (1998).
17. K. Okano, H. Naruki, Y. Akiba, T. Kurosu, M. Lida, Y. Hirose. Jpn. J. Appl. Phys. **27**, L173 (1988).
18. H. B. Martin, A. Argoitia, U. Landau, A. B. Anderson, J. C. Angus. J. Electrochem. Soc. **143**, L133 (1996).
19. A. Ya. Sakharova, Yu. V. Pleskov, F. Di Quarto, S. Piazza, C. Sunseri, I. G. Teremetskaya, V. P. Varnin. J. Electrochem. Soc. **142**, 2704 (1995).
20. K. Patel, K. Hashimoto, A. Fujishima. J. Photochem. Photobiol. A: Chem. **65**, 419 (1992).
21. L. Boonma, T. Yano, D. A. Tryk, K. Hashimoto, A. Fujishima. J. Electrochem. Soc. **144**, L142 (1997).
22. H. Dürr, H. Bouas-Laurent. Photochromism, Elsevier, Amsterdam, p.165 (1990)
23. Z. F. Liu, K. Hashimoto, A. Fujishima. Nature **347**, 658 (1990).
24. A. Ueno, H. Yoshimura, T. Osa. J. Am. Chem. Soc. **101**, 2779 (1979).
25. G. Klopman, N. Doddapaneni. J. Phys. Chem. **78**, 1835 (1974).
26. K. Morigaki, Z. F. Liu, K. Hashimoto, A. Fujishima. J. Phys. Chem. **99**, 14771 (1995).
27. A. Fujishima, T. N. Rao. Proc. Indian Acad. Sci. (Chem. Sci.) **109,** 471 (1997).
28. N. Negishi, T. Iyoda, K. Hashimoto, A. Fujishima. Chem. Lett. 841 (1995).
29. H. Matsubara, M. Takada, S. Koyama, K. Hashimoto, A. Fujishima. Chem. Lett. 767 (1995).
30. Y. Kikuchi, K. Sunada, T. Iyoda, K. Hashimoto, A. Fujishima. J. Photochem. Photobiol. A: Chem. **106**, 51 (1997).
31. Y. Kubota, T. Shuin, C. Kawasaki, M. Hosaka, H. Kitamura, R. Cai, H. Sakai, K. Hashimoto, A. Fujishima. Br. J. Cancer **70**, 1107 (1994).
32. Y. Ohko, K. Hashimoto, A. Fujishima. J. Phys. Chem. A. **101**, 8057 (1997).
33. Y. Ohko, A. Fujishima, K. Hashimoto. J. Phys. Chem. A. **102**, 1729 (1998).
34. A. Heller. Acc. Chem. Res. **28**, 503 (1995).
35. H. Sakai, R. Baba, K. Hashimoto, A. Fujishima, A. Heller. J. Phys. Chem. **99**, 11896 (1995).
36. K. Ikeda, H. Sakai, R. Baba, K. Hashimoto, A. Fujishima. J. Phys.Chem. **101**, 2617 (1997).
37. K. Ikeda, K. Hashimoto, A. Fujishima. J. Electroanal. Chem. **437**, 241 (1997).
38. T. N. Rao, D. A. Tryk, K. Hashimoto, A. Fujishima. Submitted for publication.
39. H. Takano, K. Morigaki, K. Hashimoto, A. Fujishima. Manuscript in preparation.